

Surface roughness analysis of ETP-CVD a-Si:H thin films deposited at high growth rates around 1 nm/s

M. A. Wank,¹ R. A. C. M. M. van Swaaij,¹ and M. C. M. van de Sanden²

¹Delft University of Technology,
DIMES-ECTM,

P. O. Box 5053, 2600 GB Delft, the Netherlands.

Phone: +31-15-2782185 E-mail: m.a.wank@tudelft.nl

²Eindhoven University of Technology,

Department of Applied Physics,

P. O. Box 513, 5600 MB Eindhoven, the Netherlands.

Abstract—The surface roughness and morphology of hydrogenated amorphous silicon (a-Si:H) thin films can have critical influence on device performance in microelectronic devices. The self-affine kinetic roughening of thin-film growth follows from a competition between roughening and smoothening mechanisms. Thus from a study of the surface roughness evolution, insight into surface mechanisms during growth and their influence on structural properties of thin films can be gained. Consequently there is a strong technological motivation to understand the origin of surface roughness and morphology. Commonly the surface roughness development is analyzed utilizing dynamic scaling theory [1]. Experimental evidence of such scaling behavior has been found for several different deposition techniques (e. g. [2], [3]). A widespread method to analyze the surface roughness development is atomic force microscopy (AFM). It delivers both lateral and vertical information on the surface roughness development. A-Si:H can be deposited at high growth rates (up to 10 nm/s) via the Expanding Thermal Plasma Chemical Vapor Deposition (ETP-CVD). In this contribution, we will analyze the surface roughness development of ETP-CVD a-Si:H deposited at growth rates around 1 nm/s for different deposition temperatures, utilizing AFM measurements, Spectroscopic Ellipsometry and dynamic scaling theory to gain insight into surface process during film deposition.

Keywords— ETP-CVD, hydrogenated amorphous silicon, spectroscopic ellipsometry

I. INTRODUCTION

The surface morphology and development during deposition of thin films is a direct result of the processes on this surface which result in film growth. Thus a study of the

surface morphology and its development during deposition allows studying fundamental growth processes during deposition, more specifically the competition between roughening and smoothening mechanisms, as well as their influence on structural and physical properties. Furthermore, the surface roughness of hydrogenated amorphous silicon (a-Si:H) thin films can have critical influence on device performance in microelectronic devices. Consequently there is a strong technological motivation to understand the origin of surface roughness and morphology.

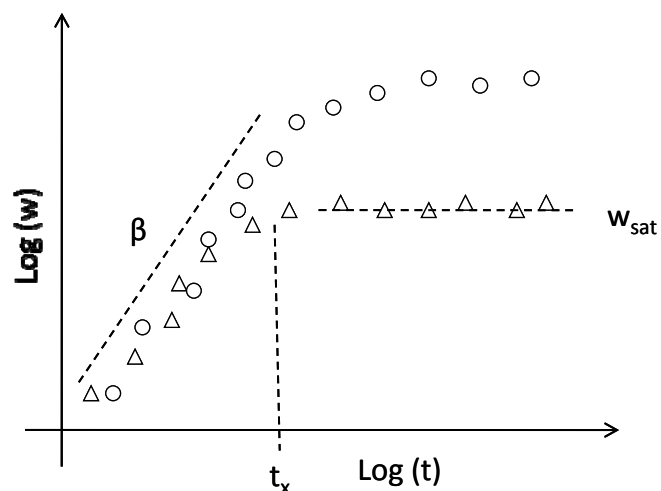


Fig. 1: Schematic overview of surface roughness development, w , versus time, t . Indicated in the figure are the growth exponent β , the crossover time t_x and the saturation roughness w_{sat} .

In order to compare different, static surfaces quantitatively and qualitatively, various statistical tools have been developed, e. g. the surface mean height, root mean square (rms) roughness, correlation length and others. Additionally, many surfaces exhibit scaling properties, which simplifies the description of a surface significantly [1]. In the most common case of self-affine scaling, vertical and horizontal features are scaled by different scaling factors to obtain surfaces that are statistically identical to the unscaled surface. In the special case where the horizontal and vertical scaling parameters are identical, we speak of self-similar scaling. Mathematical tools associated with fractals can be utilized in the concept of self-affine surfaces, therefore we also speak of fractal surfaces.

In the case of growing films with a dynamic surface morphology, a similar tool for surface analysis is utilized, the concept of dynamic scaling, which was suggested by Family and Vicsek [10]. It allows for a simplification of the dynamic surface description, while providing additional tools to compare surfaces. While dynamic scaling concepts work very well with surfaces where local processes are dominant, like surface diffusion, problems can arise when non-local processes are present [1].

Several important parameters can be determined utilizing the concepts of self-affine, fractal surfaces. Some of them are schematically represented in Fig. 1. From the rms surface roughness development, $w(L,t)$, with time we can determine the *growth exponent*, β , according to:

$$w(L,t) \sim t^\beta \quad (1)$$

Here, L is the system size and t the time. This power-law increase in roughness can be observed until a saturation regime is reached where the rms roughness is constant. The saturation value, w_{sat} , is related to the system size according to another power law:

$$w_{\text{sat}}(L) \sim L^\alpha \quad (2)$$

where α is called the *roughness exponent*. The so-called crossover time t_x at which we observe the transition from behavior (1) to behavior (2) is also related to the system size according to

$$t_x \sim L^z \quad (3)$$

with z the so-called *dynamic exponent*. The Family-Vicsek relationship establishes a relation between α and z :

$$w(L,t) \sim L^\alpha f(t/L^z) \quad (4)$$

The scaling function $f(t/L^z) = \text{constant}$ for $t \gg L^z$ and $f(t/L^z) = (t/L^z)^\beta$ for $t \ll L^z$. Additionally, for systems where the growth follows the principles of dynamic scaling it can be shown that the dynamic exponent is related to α and β according to

$$z = \alpha/\beta. \quad (5)$$

Experimental evidence of such dynamic scaling behavior has been found for several different deposition techniques (e. g. [1], [2], [3]).

We will utilize the height-height correlation function (HHCF) to determine the roughness exponent α . The height-height correlation function is defined as

$$G(r) = \langle [h(\mathbf{x}) - h(\mathbf{x} + \mathbf{r})]^2 \rangle \quad (6)$$

and typically has a region for small r -values which is proportional to $r^{2\alpha}$ and a region for large r -values which is constant. At the transition of these two regions, we can determine the correlation length, ξ , which typically scales with time according to $\xi \sim t^{1/z}$, enabling us to determine the dynamic exponent z as well.

Utilizing the three scaling exponents determined with the Family-Vicsek relationship, growth models can be grouped into different universality classes. Each class has distinct values for these exponents, which allows experimental observation of scaling exponents to be assigned to one of these classes. Some universality classes and the related exponent values are shown in Table 1.

Equation	α	β	z
Edwards-Wilkinson	~ 0	~ 0	2
KPZ	0.38	0.24	1.58
Surface Diffusion	1	0.25	4
Bulk Diffusion	0.5	0.2	3.33

Table 1: An overview of several reported universality classes and the corresponding scaling exponent values.

An increasingly utilized thin-film characterization method is spectroscopic ellipsometry. It is an optical method that measures the change of polarization of a beam of light that is reflected from the film surface. Fitting these experimental data with optical models allows the determination of material properties like the dielectric function, the film thickness or the surface roughness. In-situ SE allows studying the change of these properties during the deposition of the film. However, SE does not provide any information about the lateral size of roughness features on the surface, limiting its application in the dynamic scaling concept to the determination of the growth exponent β .

We will utilize both AFM and SE to study the surface roughness of thin a-Si:H films. In-situ results from SE are compared to AFM results measured at different times of the deposition to investigate compatibility between these techniques. Furthermore we will apply the concept of dynamic scaling to compare our scaling exponents to known universality classes.

II. EXPERIMENTAL

The deposition method utilized for the work presented in this paper is called expanding thermal plasma chemical vapor deposition (ETP-CVD). High deposition rates of up to 10 nm/s for a-Si:H thin films have been demonstrated, compared to growth rates of $\sim 1\text{-}2 \text{ \AA/s}$ obtained with conventional RF-PECVD methods [3]. A schematic representation of the reactor is shown in Fig. 2.

An Ar-H₂ plasma is created in the arc, where the gases are injected into a 2.5-mm diameter tube surrounded by six isolated copper plates. A DC-discharge is sustained between three cathodes and the grounded copper plate located at the end of the arc. While the arc operates at pressures of 0.2 to 0.5 bar, a pressure of about 0.2 mbar is maintained in the reaction chamber by two stacked root blowers during depositions. Due to the large pressure difference, the plasma expands supersonically into the reactor. After a stationary shock a few centimeters after the nozzle, the plasma continues to expand subsonically.

The precursor gas silane (SiH₄) is injected into the plasma beam via an injection ring located a few centimeters below the nozzle. SiH₄ reacts with the atomic hydrogen created in the Ar-H₂ plasma, abstracting one hydrogen atom from the SiH₄ molecule, forming silyl-radicals (SiH₃), the dominant growth radical responsible for 90% of the film growth [4]. The distance between the injection ring where the SiH₄ is injected and the substrate holder is 43 cm.

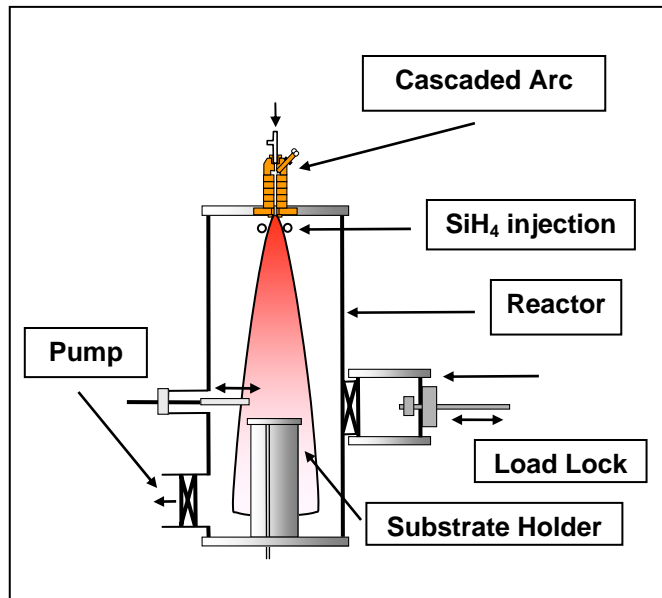


Fig. 2: Schematic drawing of the ETP-CVD reactor. The plasma is created in the arc and expands into the reactor due to the lower pressure.

For all depositions reported here, identical gas flows were used: 570 sccm Ar and 190 sccm H₂ in the arc, 150 sccm H₂ in the nozzle, and 200 sccm SiH₄ in the injection ring. The current in the arc is 40 A. The substrate temperature was varied between 150 and 300°C, deposition time was 5 minutes. The reactor pressure was around 0.15 mbar and the

deposition rate around 1.1 nm/s for all depositions. The films have been deposited on c-Si wafers (prime wafer, 500-550 μm , 2 nm native oxide).

AFM measurements were carried out with the microscope (NT-MT) in tapping mode. The tips used in these scans were silicon cantilever tips with gold reflection coating and radii of $< 10\text{nm}$. Images of the size of $2 \mu\text{m} \times 2 \mu\text{m}$ at a resolution of 512×512 pixels were recorded. Tilting of the sample surface was corrected by 1st order surface background correction. In order to avoid artifacts introduced by sample drift during the measurement, only scan lines in the fast-scan direction were utilized for the analysis.

Our RTSE measurements were performed using a J. A. Woollam Co., Inc M-2000F rotating compensator spectroscopic ellipsometer. The measurement setup and data acquisition were controlled using WVASE 3.486 provided by J. A. Woollam Co., Inc. Spectra were collected from 250 nm to 1000 nm in 470 separate channels. The angle of incidence was about 68° and the light beam passed through non-strain free windows, so a window effect had to be included in the data analysis. For all in-situ experiments 8 measurements were averaged, resulting in a time resolution of about 1.8 s. For the fitting of our experimental data we used EASE 2.3 by J. A. Woollam Co., Inc.

The actual data obtained in an RTSE measurement is the change of the polarization state of the incident light beam, defined by the ellipsometric angles Ψ and Δ as a function of wavelength. These polarization angles by themselves do not give any information about the sample structure. A fitting procedure is required to deduce physical information like layer thickness and dielectric function. Depending on the sample structure, a single or multilayer model must be created, in our case consisting of a substrate (crystalline silicon wafer) with a thin bulk film (a-Si:H) and a roughness layer, modeled by a mixture of 50% film / 50% voids, following the Bruggeman effective medium approach (EMA) [11]. In the final fitting, the only fitted parameters are the bulk film thickness, d_f , and the thickness of the surface roughness layer, d_s . In this paper, we will distinguish between the surface roughness layer thickness, d_s determined with SE, and the rms surface roughness w determined with AFM.

In our RTSE data analysis we follow a procedure similar to the one established by Van den Oever et al. [5]. The first step is to determine the dielectric function of the substrate. We follow the pseudo-substrate approach and determine the dielectric function numerically from the RTSE data directly before the deposition by numerical inversion [6]. The dielectric function of the substrate is thus obtained at the same temperature at which the deposition is carried out later and analysis problems due to the temperature dependence of the dielectric function of the substrate can be excluded.

The dielectric function of the deposited film can be modeled by parameterized models, for example Cody-Lorentz- or Tauc-Lorentz-models. However, this requires initial assumptions for the starting values of the parameters, so one must already have a good idea of the dielectric function of

the material. Additionally it introduces additional fitting parameters. The approach taken in this work does not require any parameterization of the dielectric function. Instead a tabulated, Kramers-Kronig consistent version of the dielectric function is fitted via a global regression analysis using around 8 spectra of the in-situ measurement equally distributed over the deposition time, excluding only the initial 200 Å. The fit of the dielectric function is repeated until a minimum in the mean square error (MSE) is reached. Utilizing many spectra stretched over the whole deposition time ensures a good representation of the bulk dielectric function. An initial, tabulated version is required as a starting point for the fitting procedure, as well as the dielectric function of the substrate obtained in the previous step. Surface roughness is implemented using the EMA with 50% voids.

Once the dielectric functions have been extracted, the dynamic fit of the in-situ data can be carried out. The only parameters in this final, dynamic fit are d_f and d_s .

III. RESULTS & DISCUSSION

The roughness development as it is typically observed for SE measurements is demonstrated in Fig. 3 for depositions at 200°C, 250°C and 300°C. In the early growth phase up to a total film thickness of 400Å, we observe a phase with an initial smoothing and a subsequent stronger roughening. The initial smoothing is presumably related to the coalescence of nuclei that initially form on the substrate. The strong roughening phase is a transitional stage in which long-range features evolve on the surface, which dominate the morphology in the steady growth phase that starts after the initial 400Å.

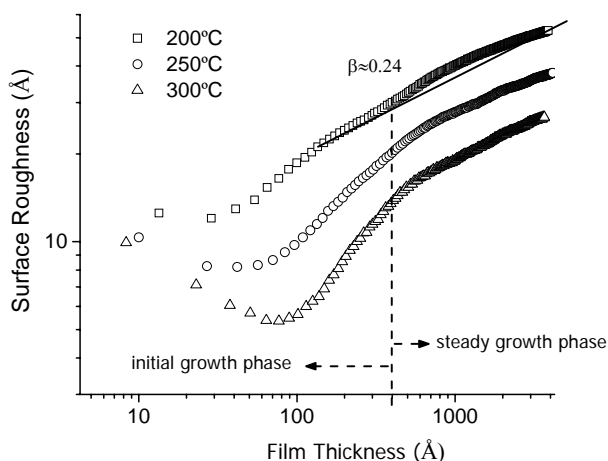


Fig. 3: Surface roughness development measured with SE for three different deposition temperatures. The solid line indicates the region where the β -value was determined.

The SE roughness development for three different temperatures shown above demonstrates the temperature-

independence observed for our β -values. For all three temperatures, we obtain values around 0.25 by fitting β according to the power law relation $d_s \sim t^\beta$. However, despite the comparable similarity of growth exponent values, we still observe a significant difference in the final roughness value. Films deposited at higher temperatures exhibit smoother surfaces at the end of the deposition. We can see that this difference in final film roughness is related to the roughness development in the initial 100Å. Films deposited at 300°C go through a much stronger smoothing phase than films deposited at lower temperatures. This is presumably related to differences in radical mobility in the early growth phase and needs to be investigated further.

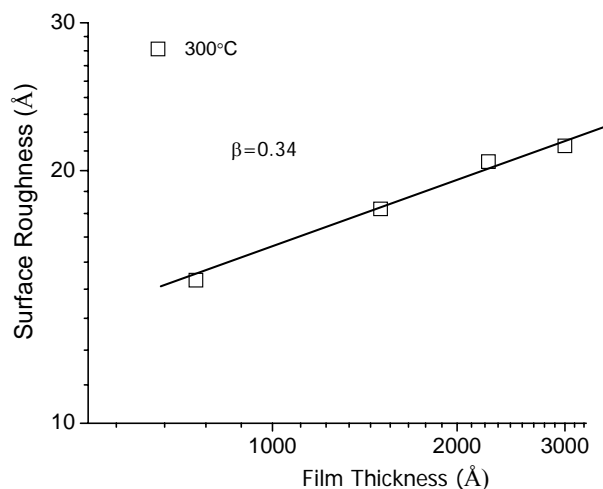


Fig. 4: The rms surface roughness development as it was determined from AFM scans for several depositions at 300°C. The solid line indicates the slope that determines the β -value.

In Fig. 4 we see the surface roughness for depositions at 300°C. In this case the roughness was determined with AFM measurements and corresponds to the statistical rms roughness. As only 4 measurements at 750Å, 1500Å, 2250Å and 3000Å were carried out, we are not able to observe the initial stage below 400Å which we observed for SE measurements in Fig. 3. Comparing the roughness obtained from SE with the rms roughness, we see that the values are comparable. At the final thickness we have an rms of 21Å and a SE roughness layer thickness around 26Å. At 800Å bulk film thickness, 17Å from SE compare even better to the rms roughness of 15Å. The difference in β compares well to the higher roughness obtained with AFM at higher film thicknesses. An increase in the difference between rms roughness and SE roughness proportional to the bulk film thickness has been reported before by Koh et al. [8]. They determined the relation between the two roughness values to be $d_s = 1.5 d_{rms} + 4 \text{ Å}$, however, for our results the factor of 1.5 appears too large, we can determine a factor around 1.25. Additionally the offset of 4Å is not present for our data.

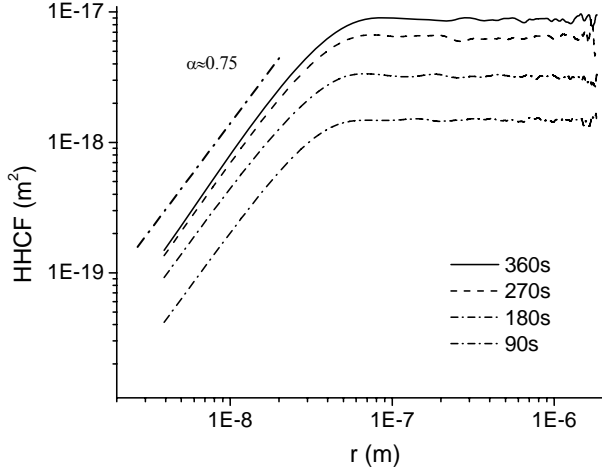


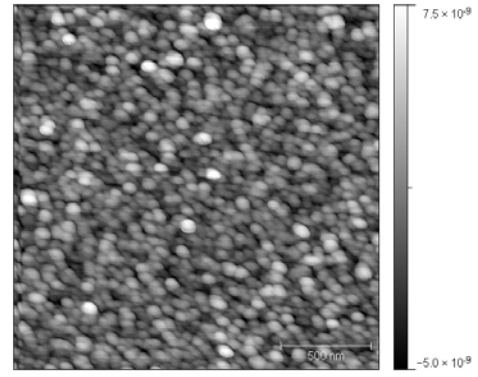
Fig. 5: Height-height correlation functions determined for four AFM scans at different stages in the deposition. The dash-dotted line indicates the slope that determines the α -value.

For both the SE (Fig. 3) and AFM measurements (Fig. 4), we have determined the growth exponent β which is indicated in the corresponding figures by solid lines. The growth exponent is slightly higher for AFM measurements, where we obtain a value of 0.34, whereas for SE measurements we determine a value of 0.25. The β value from SE measurements corresponds to the universality class called surface diffusion while the value from AFM measurements cannot be associated to any of the classical universality classes.

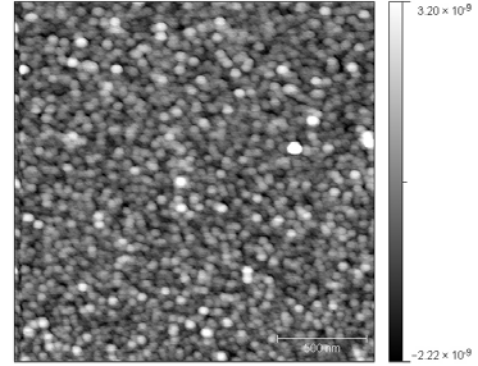
In Fig. 5 we see the height-height correlation functions $G(r)$ determined from the AFM measurements carried out at the samples from Fig. 4. For all depositions we see the typical shape of the HHCF with an initial region proportional to $r^{2\alpha}$ followed by a constant region. From the initial region we have determined the roughness exponent α to be around 0.75 for all deposition times. This value is not compatible to any of the universality classes reported in Table 1. A similar value ($\alpha = 0.87$) has been reported previously by Sperling et al [3] for a-Si:H thin film growth by hot-wire deposition.

The dynamic exponent z has been determined according to the correlation lengths ξ from Fig. 5 utilizing the relationship $\xi \sim t^{1/z}$, we obtain $z \sim 3.2$. Additionally utilizing the relationship between the exponents α , β and z determined by Family-Vicsek given in Eq. 5 we determine $z \sim 2.2$, which is not in agreement with the value obtained using the correlation length, ξ .

Our scaling exponents have been determined to be $\alpha = 0.75$, $\beta = 0.25$ (SE) respectively $\beta = 0.34$ (AFM) and $z = 3.2$. This combination of exponents does not correspond to any of the known universality classes. Additionally it violates the Family-Vicsek scaling hypothesis which requires $z = \alpha/\beta$. We can conclude that for our depositions we observe anomalous roughening. A similar observation has been made by Sperling et al. [3].



a) $t=360s$



b) $t=90s$

Fig. 6: AFM images ($2 \mu\text{m} \times 2 \mu\text{m}$) of a-Si:H surfaces at two different stages in the deposition process.

In Fig. 6 we can see two AFM images at $2 \mu\text{m} \times 2 \mu\text{m}$ scan size at a resolution of 512×512 pixels. The images have been taken for depositions at 300°C at 90s and 360s of deposition time. The morphology of the surface is clearly random with no obvious pattern formation. Both the lateral and vertical size of surface features increase with deposition time, although the increase in vertical size is more pronounced than the increase in lateral size. This observation corresponds well to the height-height correlation function shown in Fig. 5, where we observe a similar increase in ξ with deposition time as well as an increase in the saturation width of surface roughness $G(r \gg \xi)$.

IV. CONCLUSION

We have determined the scaling exponents for a-Si:H deposited with ETP-CVD at growth rates around 1nm/s to be $\alpha = 0.75$, $\beta = 0.25$ (SE), respectively $\beta = 0.34$ (AFM), and $z = 3.2$. Our results violate the Family-Vicsek scaling hypothesis and do not comply with any known universality classes, thus representing anomalous scaling. The roughness development obtained via AFM differs from that obtained via SE. We obtain stronger rms roughening, resulting in a larger growth exponent for our AFM measurement.

ACKNOWLEDGEMENTS

Kasper Zwetsloot and Martijn Tijssen are acknowledged for their skilful technical assistance. This research was financially supported by SenterNovem.

REFERENCES

- [1] A.-L. Barabasi and H. E. Stanley, *Fractal Concepts in Surface Growth*, Cambridge University Press, Cambridge, U.K., 1995.
- [2] A. H. M. Smets, W. M. M. Kessels, and M. C. M. van de Sanden, *Appl. Phys. Lett.* **82**, 865 (2003).
- [3] B. A. Sperling, J. R. Abelson, *J. Appl. Phys.* **101**, 024915 (2007).
- [4] W. M. M. Kessels, Ph. D. Thesis, Eindhoven University of Technology (2000).
- [5] W. M. M. Kessels, A. Leroux, M. G. H. Boogaarts, J. P. M. Hoefnagels, M. C. M. van de Sanden, and D. C. Schram, *J. Va. Sci. Technol. A.* **19**, 467 (2001).
- [6] P. J. van den Oever, M. C. M. van de Sanden, W. M. M. Kessels, *J. Appl. Phys.* **101** (2007).
- [7] H. Arwin, D. E. Aspnes, *Thin Solid Films* **113**, 101 (1984)
- [8] M. Pelliccione, T. M. Lu, *Modern Physics Letters B*, Vol. **21**, 1207-1225, (2007)
- [9] J. Koh, Y. Lu, C. R. Wronski, Y. Kuang, R. W. Collins, T. T. Tsong, Y. E. Strausser, *Appl. Phys. Lett.* **69**, 1297 (1996).
- [10] F. Family and T. Vicsek, *J. Phys. A* **18**, L75 (1985).
- [11] H. Fujiwara, J. Koh, P. I. Rovira, and R. W. Collins, *Phys. Rev. B* **61**, 10832 (2000).